New Phytologist

Research

Meiocyte size is a determining factor for unreduced gamete formation in *Arabidopsis thaliana*

Jun Yi[1], David Kradolfer[1], Lynette Brownfield[2], Yingrui Ma[3], Ewa Piskorz[3], Claudia Köhler[1,4] and Hua Jiang[3]

[1]Department of Plant Biology, Uppsala BioCenter, Linnean Center for Plant Biology, Swedish University of Agricultural Sciences, Uppsala, SE-75007, Sweden; [2]Department of Biochemistry, University of Otago, Dunedin, 9054, New Zealand; [3]Leibniz Institute of Plant Genetics and Crop Plant Research, Gatersleben 06466, Germany; [4]Max Planck Institute of Molecular Plant Physiology, Potsdam-Golm, 14476, Germany

Authors for correspondence:
Claudia Köhler
Email: koehler@mpimp-golm.mpg.de

Hua Jiang
Email: jiangh@ipk-gatersleben.de

Received: *3 March 2022*
Accepted: *24 August 2022*

New Phytologist (2023) **237:** 1179–1187
doi: 10.1111/nph.18473

Key words: 2n pollen, *Arabidopsis thaliana*, chromosome separation, meiosis, polyploidization, the organelle band.

Summary

- Polyploidy, the presence of more than two sets of chromosomes within a cell, is a widespread phenomenon in plants. The main route to polyploidy is considered through the production of unreduced gametes that are formed as a consequence of meiotic defects. Nevertheless, for reasons poorly understood, the frequency of unreduced gamete formation differs substantially among different plant species. The previously identified meiotic mutant *jason* (*jas*) in *Arabidopsis thaliana* forms about 60% diploid (2n) pollen. JAS is required to maintain an organelle band as a physical barrier between the two meiotic spindles, preventing previously separated chromosome groups from uniting into a single cell.
- In this study, we characterized the *jas* suppressor mutant *telamon* (*tel*) that restored the production of haploid pollen in the *jas* background.
- The *tel* mutant did not restore the organelle band, but enlarged the size of male *jas tel* meiocytes, suggesting that enlarged meiocytes can bypass the requirement of the organelle band. Consistently, enlarged meiocytes generated by a tetraploid *jas* mutant formed reduced gametes.
- The results reveal that meiocyte size impacts chromosome segregation in meiosis II, suggesting an alternative way to maintain the ploidy stability in meiosis during evolution.

Introduction

Meiosis is a reductive cell division where a single round of DNA replication is followed by two consecutive chromosome divisions, generating cells carrying half the amount of the parental chromosomes (Ma, 2006; Zamariola *et al.*, 2014). In flowering plants (angiosperms), male and female meiosis takes place in anthers and ovules, respectively. The products of male and female meiosis, microspores and megaspores respectively, have different fates. After male meiosis, all microspores survive and develop into mature pollen (Hamamura *et al.*, 2012). By contrast, in most angiosperms only one functional megaspore is produced that develops into a seven-celled mature female gametophyte, containing two gametes, the haploid egg cell and the central cell. After pollination, male and female gametes fuse in a process termed double fertilization, leading to the formation of the embryo and the endosperm (Bleckmann *et al.*, 2014). Proper execution of meiosis is essential for plant reproduction. Defects in meiosis typically result in imbalanced gametes, manifested in premature spore abortion and sterility. However, meiotic failure can also lead to viable unreduced gametes containing somatic chromosome numbers (Brownfield & Kohler, 2011). The *jason* (*jas*) mutant forms unreduced (2n) male gametes at high frequency due to a disordered spindle orientation at metaphase II. This causes chromosomes that have been separated in meiosis I to come close again at anaphase II, generating two diploid cells that contain non-sister chromosomes (d'Erfurth *et al.*, 2008; Erilova *et al.*, 2009; Li *et al.*, 2010; De Storme & Geelen, 2011; Brownfield *et al.*, 2015).

Thus, spindle polarity and orientation is essential for chromosome separation in plants, especially in the majority of dicotyledonous plants that undergo simultaneous male meiotic cytokinesis, where cytokinesis only occurs only after the completion of the second round of chromosome division (Brownfield & Kohler, 2011; De Storme & Geelen, 2013). Without the intervening cytokinesis after meiosis I, bi-orientated, physically separated spindles correctly segregate chromosomes by a tetrahedral arrangement into four haploid cells following meiosis II (Zamariola *et al.*, 2014). Recent work revealed that the organelle band establishes a physical barrier maintaining the segregation of two spindles (Brownfield *et al.*, 2015). Typically, at the end of meiosis I, organelles aggregate at the equator of meiotic cells, forming an organelle band. While the organelle band also forms in *jas*, it becomes disrupted early in meiosis II, before disordered spindle

© 2022 The Authors
New Phytologist © 2022 New Phytologist Foundation.
This is an open access article under the terms of the Creative Commons Attribution License, which permits use, distribution and reproduction in any medium, provided the original work is properly cited.

Check for updates

14698137, 2023, 4, Downloaded from https://nphonlinelibrary.wiley.com/doi/10.1111/nph.18473 by Swedish University Of Agricultural Sciences, Wiley Online Library on [13/03/2023]. See the Terms and Conditions (https://onlinelibrary.wiley.com/terms-and-conditions) on Wiley Online Library for rules of use; OA articles are governed by the applicable Creative Commons License

orientation is noticeable. The loss of the organelle band likely causes free movement of spindles and a decrease in spindle separation, resulting in two groups of chromosomes from different spindles coming into close proximity at the end of meiosis II, and subsequently being incorporated into a single cell (Brownfield *et al.*, 2015). Altered organelle organization in *jas* occurs before disturbances of spindle position, indicating that JAS maintains organelle position in male meiosis but does not have a direct role in spindle organization. Consistently, JAS is co-localized with markers of the endomembrane system in the organelle band rather than being associated with the spindle (Brownfield *et al.*, 2015).

In this paper, we aimed at identifying the role of the organelle band during male meiosis. We discovered that the presence of the organelle band is not required in enlarged meiocytes in the *jas* suppressor mutant *telamon* (*tel*). Consistently, enlarged meiocyte size by tetraploidization also suppressed the production of unreduced gametes, consistent with the idea that meiocyte size is crucial for determining the frequency of unreduced gamete formation.

Materials and Methods

Plant material and growth conditions

All wild-type and mutant plants were in the *Arabidopsis thaliana* accession Columbia (Col-0) background, except jas-1 in the Landsberg (Ler) background. After stratification for 3 d at 4°C, plates with *A. thaliana* seeds were transferred to a growth chamber (16 h : 8 h, light : dark; 110 µmol s^{-1} m^{-2}; 18°C; 70% humidity). After 10 d, seedlings were transferred to soil and grown in a growth chamber (16 h : 8 h, light : dark; 110 µmol s^{-1} m^{-2}; 21°C; 70% humidity). The *tel-1* mutant was isolated in a suppressor screen of the *jas-3* mutant (*Telamon* suppresses unreduced gamete formation in *jason*; Kradolfer *et al.*, 2013). The *tel-2* mutant contains a T-DNA (GABI_405C03) that disrupts the open reading frame at amino acid 189. If not otherwise indicated, *tel-1* was used for all experiments. Tetraploid *jas-3* was generated by colchicine treatment as previously described (Batista *et al.*, 2019). The *jas-1*, *atps1-1*, and *osd1-1* mutants were previously described (d'Erfurth *et al.*, 2008, 2009; Erilova *et al.*, 2009).

Ethyl methanesulfonate (EMS) mutagenesis and mapping

Ethyl methanesulfonate mutagenesis was carried out as previously described (Kradolfer *et al.*, 2013). Diploid *jas-3* seeds were selected based on seed size and mutagenized for 15 h in 0.3% EMS. The seeds were germinated on soil, and one side branch of each plant was harvested. The *jason* mutant frequently generates 2n pollen and triploid (3×) seeds upon self-fertilization (Erilova *et al.*, 2009). Triploid seeds usually collapse in the *Arabidopsis* Columbia (Col-0) accession due to the triploid block (Schatlowski & Kohler, 2012). Hence, the percentage of collapsed seeds in the *jas-3* mutant can be an indication of the portion of 2n pollen. To identify the genes required for 2n gamete formation, we first screened *c.* 1000 M2 families, each consisting of eight individuals derived from one M1 plant, for mutants that showed reduced seed abortion rates in the presence of the *jas* mutation. Afterward, we screened the suppressors for mutants that have increased proportions of 1n pollen. Since 2n pollen is significantly larger than 1n pollen (Ramsey & Schemske, 1998), we utilized the pollen size as indication of the ploidy. We compared the size of pollen in the suppressors with the size of pollen in the *jas-3* mutant to isolate suppressors that produce a reduced amount of 2n pollen. We finally identified two mutants that strongly suppressed the production of 2n pollen, one of which is *telamon (tel)*.

For genetic mapping of the *tel* mutation, we established an F2 mapping population by crossing *jas-3 tel* with *jas-1* (L*er*). We selected 200 plants with the *tel* phenotype for mapping. Leaf samples of all plants were pooled and DNA was extracted using the Nucleon PhytoPure Kit (Amersham Biosciences). Sequencing, mapping and mutant identification was carried out as previously described (Kradolfer *et al.*, 2013).

Generation of plasmids and transgenic lines

For the generation of the *ProTEL:TEL*$^{D\ to\ N}$ construct, the promoter and genomic sequence of *TEL*$^{D\ to\ N}$ were amplified from genomic DNA of *tel-1* −/− by PCR using primers specified in supporting information Table S1. The PCR products were cloned into pENTR/D-TOPO (Invitrogen) followed by integrating into the destination vector pB7WG0 with LR clonase reaction. For the generation of the *UBQ10::TEL-GFP* and *UBQ10:TEL*$^{D\ to\ N}$ constructs, the CDS sequence of *TEL* and *TEL*$^{D\ to\ N}$ was amplified from the cDNA of Col and *tel-1* −/− and was cloned into pENTR/D-TOPO (Invitrogen). TEL-pENTR and TEL$^{D\ to\ N}$-pENTR were cloned into the pUBC-GFP vector (Grefen *et al.*, 2010) by LR clonase reaction.

Microscopic and phenotypic analyses

The analysis of meiocytes located in the anther was performed according to the published protocol (Rossig *et al.*, 2021). Briefly, inflorescences with closed buds were fixed overnight in 3 : 1, ethanol : acetic acid. Anthers with meiocytes were directly placed on a microscope slide and stained with 4′,6-diamidino-2-phenylindole (DAPI) (0.4 µg ml^{-1}) in phosphate buffer (100 mM sodium phosphate (pH 7.0), 1 mM EDTA and 0.1% Triton X-100) for 5 min. Then the material was covered and directly viewed under a Zeiss 780 Confocal Laser Scanning Microscope. The wavelength of 415–470 nm was used for detecting the DAPI signal. The settings were adjusted so that organelle DNA could be clearly seen, which resulted in genomic DNA signals becoming saturated. While multiple anthers are on each slide, the stages of interest (metaphase II) are of short duration. Slides were screened for anther locules containing this stage (locules are not all synchronised, Rossig *et al.*, 2021). Within anther locules containing male meiocytes at metaphase II, only meiocytes with two clear groups of chromosomes were chosen for imaging and measurement. The 'Line' function in the Graphic manual bar of the Zeiss confocal software ZEN was used to

© 2022 The Authors
New Phytologist © 2022 New Phytologist Foundation.

14698137, 2023, 4, Downloaded from https://nphonlinelibrary.wiley.com/doi/10.1111/nph.18473 by Swedish University Of Agricultural Sciences, Wiley Online Library on [13/03/2023]. See the Terms and Conditions (https://onlinelibrary.wiley.com/terms-and-conditions) on Wiley Online Library for rules of use; OA articles are governed by the applicable Creative Commons License

14698137, 2023, 4, Downloaded from https://nphonlinelibrary.wiley.com/doi/10.1111/nph.18473 by Swedish University Of Agricultural Sciences, Wiley Online Library on [13/03/2023]. See the Terms and Conditions (https://onlinelibrary.wiley.com/terms-and-conditions) on Wiley Online Library for rules of use; OA articles are governed by the applicable Creative Commons License

measure the distance between chromosomes. The vertical distance between two groups of chromosomes was defined as chromosome distance. The function of 'Spline Contour' at the Graphic manual bar was used to measure the size of meiocytes. The focus was adjusted to ensure that the largest area was taken for each meiocyte. To normalize the variation between different cells, male meiocytes from at least three locules were measured to generate the boxplot. The significance of difference was tested by Kolmogorov–Smirnov test.

To analyse male meiotic products, flower buds were fixed at stage 9 (Armstrong & Jones, 2003) in 3 : 1, ethanol : acetic acid solution. Floral buds were squashed on a slide and the callose cell wall of male meiotic products was stained by some drops of aniline blue solution (0.1% (m/v) in 0.033% K_3PO_4 (m/v)). For the analysis of cell size in roots, seeds were dispersed on ½-strength Murashige & Skoog medium and stratified at 4°C for 3 d. Seeds were germinated at 22°C under standard conditions for 4 to 6 d. For measuring cell size, seedlings were stained with 10 μg ml^{-1} propidium iodide (PI) (Sigma-Aldrich) for 2 min. The GFP signal was visualized under a Zeiss 780 Confocal Laser Scanning Microscope, using wavelengths of 500–550 nm and the signal of Hoechst staining was visualized using wavelengths of 610 to 630 nm. The significance of difference was determined using a Kolmogorov–Smirnov test.

For detecting the GFP signal, suspensions of *A. tumefaciens* (strain GV 3101) were infiltrated into leaves of *Nicotiana benthamiana* as described previously (Martin *et al.*, 2009). At 24 h after infiltration, water-mounted sections of leaf tissue were examined by confocal microscopy (LSM 710; Zeiss). The GFP signal was visualized using wavelengths of 500–550 nm.

Results

Telamon suppresses unreduced gamete formation in *jason*

To identify genetic factors impacting on unreduced gamete formation, we screened for suppressors of the *jas* phenotype. The *jas* mutant forms 2n pollen at high frequency (*c.* 60%), while female meiosis is not affected. We generated a mutagenized population of diploid *jas-3* plants and screened for mutants with a reduced rate of 2n pollen. Self-fertilization in *jas-3* plants results in the formation of diploid and triploid (3×) seeds (Erilova *et al.*, 2009; De Storme & Geelen, 2011). As triploid seeds usually collapse in the *Arabidopsis* Col accession because of the triploid block; we first screened for reduced rates of collapsed seeds in the *jas* mutant as a measure for reduced 2n pollen formation. As suppressors of triploid seed abortion would also give rise to increased number of viable seeds, we re-screened mutants with reduced seed collapse for a reduced rate of 2n pollen based on the meiotic products produced. We identified one mutant that strongly suppressed 2n pollen formation, which we named *telamon* (*tel*) after one of the Argonauts who sailed alongside Jason in the quest for the golden fleece. The *jas tel* mutant had fewer aborted seeds than *jas* (Fig. 1a,b), and the reduction in seed abortion in *jas tel* was accompanied by a reduction in the number of unreduced gametes. The *jas* mutant forms *c.* 40% dyads and 40% triads, of which all microspores from dyads and one-third from triads develop into 2n pollen; these numbers were reduced to *c.* 20% triads and < 5% dyads in the *jas tel* mutant (Fig. 1c–f). This revealed that *tel* acts as a suppressor of the male meiotic defect of *jas*. Homo- and heterozygous *tel* mutants caused the same phenotype (Fig. 1f), indicating that *tel* is a dominant mutant. We addressed whether *tel* could also suppress the meiotic defect of the *osd1* and *atps1* mutants, which also generate 2n pollen at high frequency (d'Erfurth *et al.*, 2008, 2009). The number of dyads and triads in *osd1 tel* and *atps1 tel* double mutants did not significantly differ from those of the single mutants (Fig. 1f), revealing that *tel* acts as a specific suppressor for *jas*, but not for *atps1* and *osd1*.

The *tel* mutation enlarges *jas* meiotic cells

The *jas* mutant has a defect in the organelle band, causing separated chromosome groups to unite again in meiosis II, resulting in the formation of dyads and triads (Brownfield *et al.*, 2015). Given that *tel* suppressed the formation of abnormal meiotic products in *jas*, we tested if the loss of the organelle band was reversed by *tel*. We used confocal laser scanning microscopy (CLSM) to view DAPI-stained meiocytes within the anther locule. During meiosis II, chromosomes aligned in metaphase II in both, wild type and *jas*. In wild-type meiocytes, the organelle band separated the two chromosome groups at metaphase II (Fig. 2a), while in *jas* meiocytes the disrupted organelle band enabled chromosome groups to move close together and even become parallel (Fig. 2b). In *jas tel* meiocytes, the chromosome groups remained well separated at metaphase II, despite the organelle band remaining disrupted as in *jas* (Fig. 2c). Hence, restored tetrad formation by *tel* is not dependent on the restoration of the organelle band, indicating a novel mechanism for maintaining spindle separation in meiosis II.

The size of *jas tel* meiocytes was noticeably larger than in wild type and *jas* (Fig. 2a–d). This was reflected by an increased distance between the two chromosome groups in *jas tel* compared to *jas* at metaphase II, that was even larger than in wild-type meiocytes (Fig. 2e). This data suggests that the enlarged meiocyte size and the resulting increased distance between the chromosome groups maintains spindle separation in the absence of the organelle band. To address whether increased meiocyte size in *jas tel* depends on the *jas* mutation, we measured the size of *tel* male meiocytes without the *jas* mutation. Interestingly, male *tel* meiocytes were not substantially larger than wild-type meiocytes (Fig. 2d). Likewise, the distance between the chromosome groups was not substantially increased in *tel* compared to wild type (Fig. 2e), indicating that *tel* enlarged male meiocytes when *JAS* was mutated. We also tested whether the increase in cell size in *jas tel* could be observed in sporophytic cells. However, the size of *jas tel* mature root cortex cells was not significantly larger compared to wild type (Kolmogorov–Smirnov test, $P = 1$), suggesting that the effect of *tel* is restricted to male *jas* meiocytes (Fig. 2f). Together, we propose that the *tel*-mediated increase in meiocyte size allows spindles to maintain separation from each other, independently of the presence of the organelle band.

© 2022 The Authors
New Phytologist © 2022 New Phytologist Foundation.

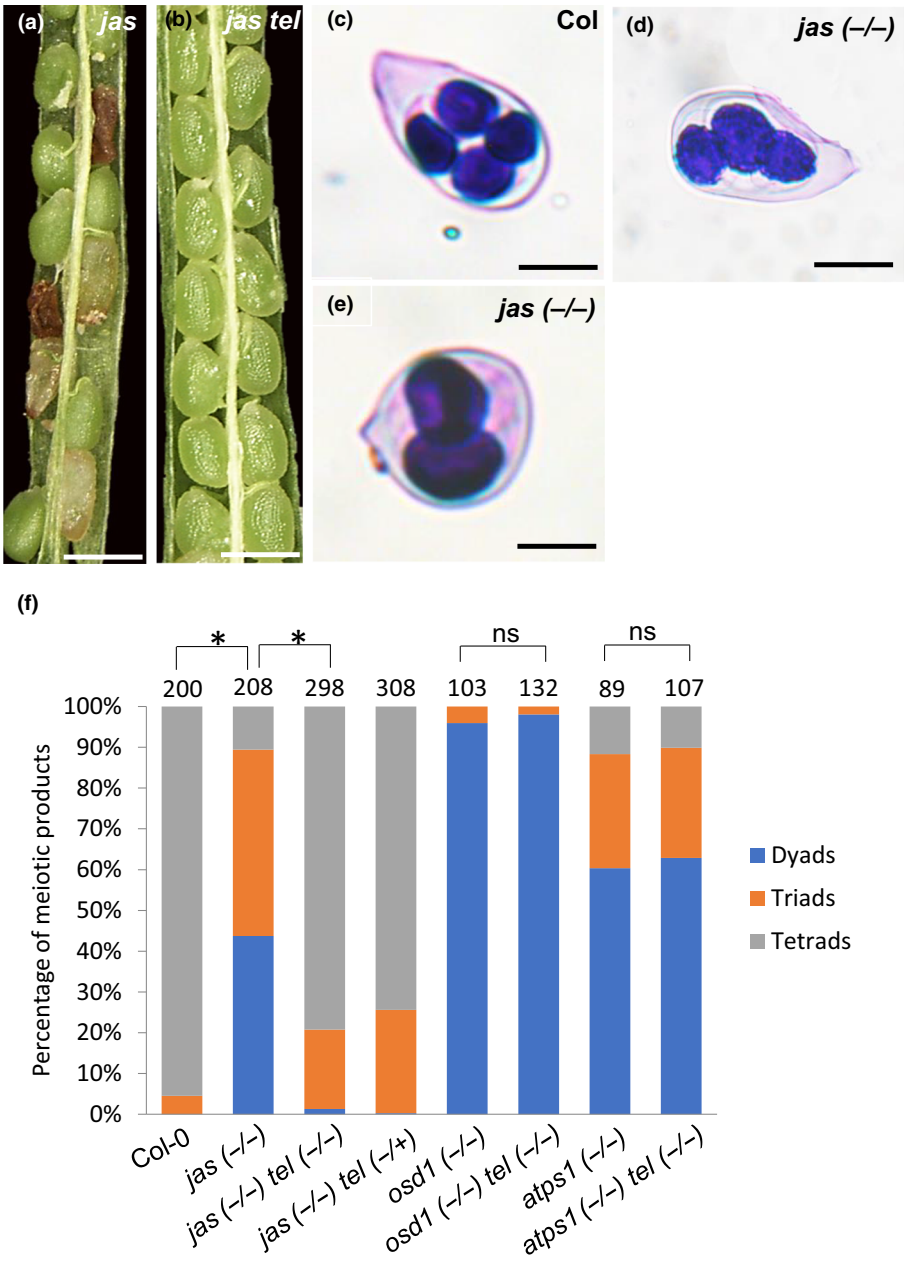

Fig. 1 In *Arabidopsis thaliana*, the *telamon* (*tel*) *(−/−)* mutant suppresses unreduced gamete formation in *jason* (*jas*). (a) A silique from *jas (−/−)* with some collapsed brown seeds. (b) A silique from *jas (−/−) tel (−/−)* containing normal seeds. Bar, 500 μm. (c–e) Different meiotic products observed in *jas*. Bar, 100 μm. (c) Dyad. (d) Triad. (e) Tetrad. Bar, 10 μm. (f) Percentage of dyads, triads, and tetrads in different genotypes. Significance of the differences was tested by Chi-square test. Asterisks mark significance ($P < 1.0\,e{-}40$), ns, not significant. Numbers above indicate number of meiotic products observed.

The organelle band is not required for chromosome segregation in enlarged meiocytes

Polyploidization is frequently associated with increased cell and organ size (Orr-Weaver, 2015). To test the hypothesis that enlarged meiocytes can separate chromosome groups in meiosis II in the absence of the organelle band, we generated tetraploid (4×) *jas* mutants by colchicine treatment. The organelle band was still disturbed in 4× *jas* meiocytes at metaphase II, revealing that polyploidization did not affect the organelle band (Fig. 3a,b). 4× *jas* meiocytes were significantly larger than 2× *jas* meiocytes (Kolmogorov–Smirnov test, $P = 0$), even exceeding the size of 2× *jas tel* meiocytes (Fig. 3c). Similar to the increased distance of chromosome groups caused by the *tel* mutation, the distance between chromosome groups was also significantly increased in 4× *jas* meiocytes compared to 2× *jas* (Kolmogorov–Smirnov test, $P = 0$) (Fig. 3d). Consistent with our hypothesis that enlarged meiocyte size can bypass the requirement of the organelle band, 4× *jas* formed significantly fewer dyads and triads compared to the 2× *jas* mutant, resembling the 2× *jas tel* mutant (Fig. 3e). The percentage of triads and dyads in 4× *jas* was slightly higher than in 2× *jas tel*, consistent with the closer distance of chromosome groups in 4× *jas* than in 2× *jas tel*. Together we conclude that increased meiocyte size can suppress the *jas* mutant phenotype and allows the formation of reduced gametes in the absence of the organelle band. Moreover, this data supports the notion that the *tel*-mediated suppression of the *jas* phenotype is a consequence of increased meiocyte size in *tel*.

© 2022 The Authors
New Phytologist © 2022 New Phytologist Foundation.

14698137, 2023, 4, Downloaded from https://nphonlinelibrary.wiley.com/doi/10.1111/nph.18473 by Swedish University Of Agricultural Sciences, Wiley Online Library on [13/03/2023]. See the Terms and Conditions (https://onlinelibrary.wiley.com/terms-and-conditions) on Wiley Online Library for rules of use; OA articles are governed by the applicable Creative Commons License

14698137, 2023, 4, Downloaded from https://nphonlinelibrary.wiley.com/doi/10.1111/nph.18473 by Swedish University Of Agricultural Sciences, Wiley Online Library on [13/03/2023]. See the Terms and Conditions (https://onlinelibrary.wiley.com/terms-and-conditions) on Wiley Online Library for rules of use; OA articles are governed by the applicable Creative Commons License

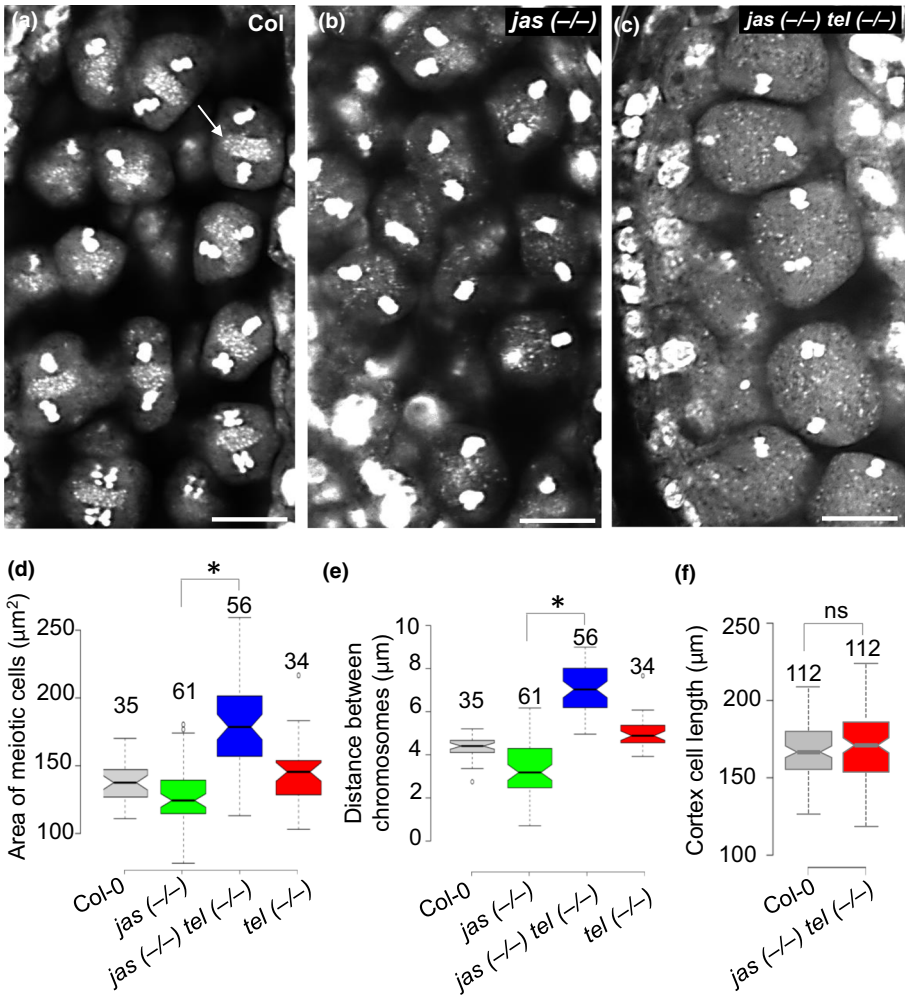

Fig. 2 In *Arabidopsis thaliana*, the *jason* (*jas*) *telamon* (*tel*) mutant has enlarged meiotic cells. (a–c) Chromosomal and organelle DNA (smaller spots) of male meiocytes in anthers stained with 4′,6-diamidino-2-phenylindole (DAPI) from Columbia (Col-0) Col wild-type (a), *jas* (−/−) (b), and *jas* (−/−) *tel* (−/−) (c) plants viewed by confocal laser scanning microscope (CLSM). Bar, 10 µm. Arrow in (a) indicated the organelle band. To clearly see the distribution of organelles, DAPI at chromosomes were overexposed. (d, e) Box plots showing the median size of meiocytes (d) and the distance between the two chromosome groups (e) at metaphase II from anthers stained with DAPI of wild-type, *jas*, and *jas tel* plants. (f) Box plot showing the median length of mature cortex cells (1st to 7th cells, both sides, 112 cell each) in Col wild-type and *jas tel* plants. The difference is not significant (Kolmogorov–Smirnov test, $P = 1$). The lower and upper hinges of the boxplots correspond to the first and third quartiles of the data, the black lines within the boxes mark the median, whiskers represent Minimum and Maximum, and circles represent outliers. Asterisks mark significance ($P < 1.0\,e{-}40$), ns; not significant. Numbers above indicate number of cells observed.

The organelle band is maintained in natural tetraploid species

If the functional requirement of the organelle band depends on the size of male meiocytes, we wondered whether big meiocytes of natural tetraploids still maintain the organelle band. To address this question, we observed male meiosis in the natural 4× *Arabidopsis* accession Wa-1 (Henry *et al.*, 2005). We could observe the ring structure of organelles surrounding chromosomes in meiosis I like in meiocytes of 2× *A. thaliana* (Fig. S1a) (Brownfield *et al.*, 2015). After finishing the first round of chromosome division, the organelle band was present at metaphase II (Fig. S1b), separating the chromosomes during the second round of division. Thus, the organelle band is still maintained in male meiocytes of 4× Wa-1.

The Wa-1 accession is one of the few natural tetraploids in *A. thaliana* with localized distribution (Novikova *et al.*, 2018) and the structure of male meiocytes of Wa-1 may not be typical for tetraploids. We therefore also investigated male meiosis in 4× *Arabidopsis arenosa* that is widely distributed across much of Northern and Central Europe (Arnold *et al.*, 2015). Nevertheless, in *A. arenosa* meiocytes the organelle ring and organelle band formed at metaphase I and II, respectively (Fig. S1c,d), like in 2× Col-0 and 4× Wa-1. While 4× *A. thaliana* and 4× *A. arenosa* accessions have a rather recent origin, *c.* 20 kya (Novikova *et al.*, 2018), the allopolyploid *C. bursa-pastoris* originated *c.* 200–300 kya (Douglas *et al.*, 2015). Also in *C. bursa-pastoris* meiocytes, we observed a similar organelle band as in the other species (Fig. S1e,f). This data suggests that, despite the function of the organelle band potentially not being required to keep spindles separated in meiosis II in tetraploids, it is nevertheless maintained over recent evolutionary timescales.

TEL encodes an F-box domain-containing protein

To identify the *tel* mutation, we crossed *jas-3 (−/−) tel (+/−)* with *jas-1 (+/−)* (L*er*) and generated an F2 mapping population to screen for plants with reduced collapsed seeds. Using mapping by sequencing, we identified the *tel* mutation to cause an amino acid substitution in gene *At2g14290* (Fig. 4a), encoding for a protein belonging to the diverse family of F-box proteins (FBPs; Xiao & Jang, 2000). F-box proteins are characterized by the presence of a loosely conserved F-box motif of *c.* 40–60 amino acids at the N-terminus and diverse C-terminal motifs. FBPs are part of SCF (Skp, Cullin, F-box) complexes, a class of E3 ubiquitin ligases targeting a variety of proteins for ubiquitin-mediated

© 2022 The Authors
New Phytologist © 2022 New Phytologist Foundation.

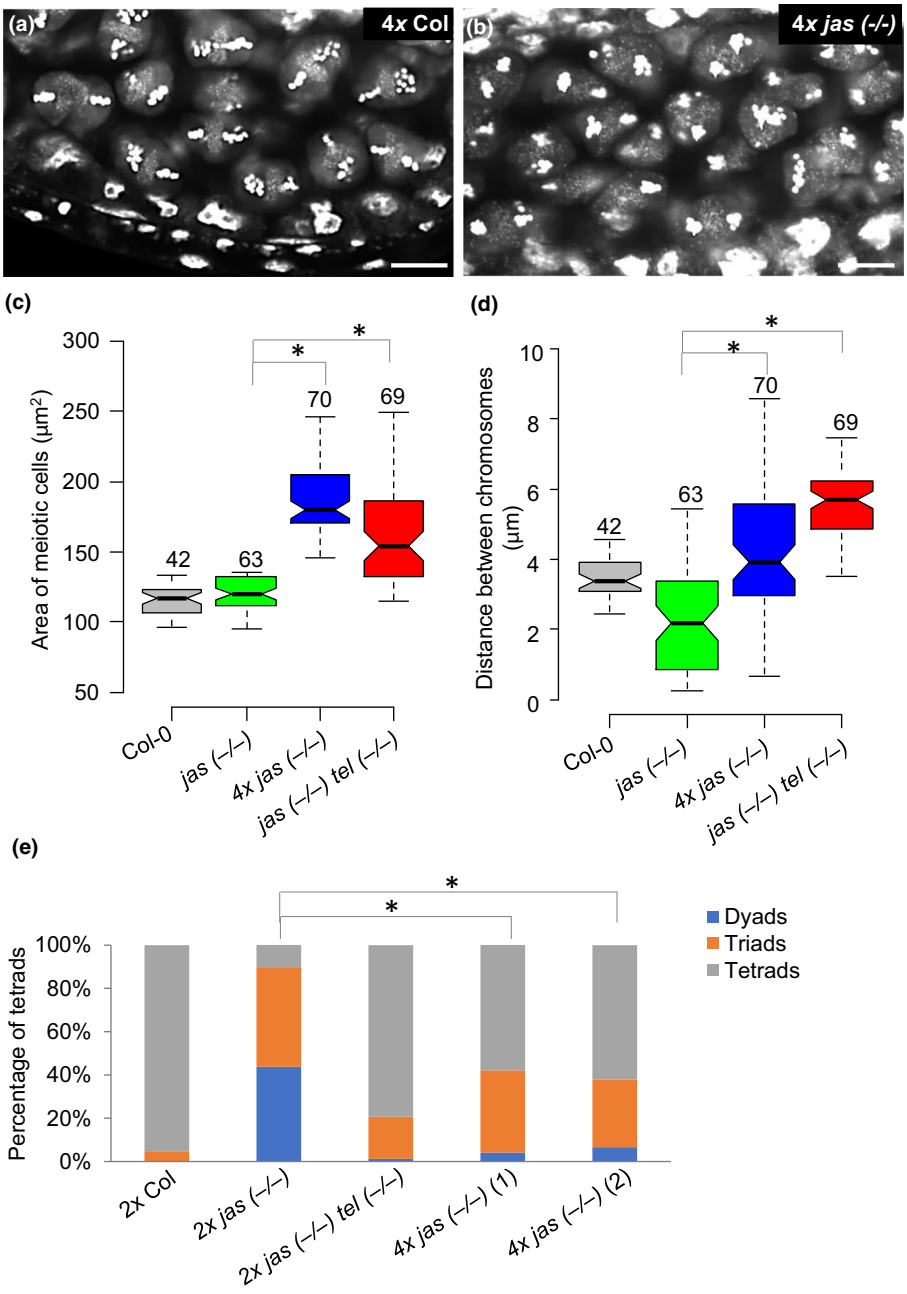

Fig. 3 In *Arabidopsis thaliana*, the tetraploid *jason* (*jas*) *(–/–)* mutant forms reduced pollen. (a, b) Chromosomal and organelle DNA (smaller spots) of male meiocytes in anthers stained with 4′,6-diamidino-2-phenylindole (DAPI) from 4× Columbia (Col-0) (a) and 4× *jas* (b) plants viewed by CLSM. Bar, 10 µm. (c, d) Box plots showing the median size (c) and distance between the two chromosome groups (d) at metaphase II in meiocytes from anthers stained with DAPI from 2× Col, 2× *jas (–/–)* and 2× *jas (–/–) telamon* (*tel*) *(–/–)*, and 4× *jas (–/–)* plants. The lower and upper hinges of the boxplots correspond to the first and third quartiles of the data, the black lines within the boxes mark the median, and whiskers represent Minimum and Maximum. Asterisks mark significance (Kolmogorov–Smirnov test). Numbers above indicate number of meiotic cells observed. (e) Percentage of dyads and triads in Col, *jas (–/–)*, *jas (–/–) tel (–/–)*, and 4× *jas (–/–)* plants. The difference between 2× *jas (–/–)* and 4× *jas (–/–)* is significant (Chi-square test, *, $P < 1.0\,e{-}40$).

degradation via the 26S proteasome pathway (Cardozo & Pagano, 2004). At2g14290, also known as FDB13, is one of 38 proteins identified in a Brassicaceae-specific family that contains an N-terminal F-Box domain and a C-terminal DUF295 domain (Fig. 4a; Lama *et al.*, 2019). The *tel* mutation caused an aspartate to asparagine (D to N) conversion at position 171 of the TEL protein, which is outside the F-box motif. Based on the prediction using Alphafold (Jumper *et al.*, 2021; Varadi *et al.*, 2022), the D171N mutation is located in a region with a very high confidence score (pLDDT > 90, Fig. 4b). The mutation is predicted to reduce the electrostatic interaction between 171D and 168K, potentially increasing the distance between the amino acid side chains and resulting in the formation of an enlarged pocket (Fig. 4c). The area including 171D and 168K is commonly conserved among the FDB family in *A. thaliana* (Table S2). Moreover, this area also showed a high level of conservation among Brassicaceae species. Interestingly, we found several proteins containing instead of the KXXD motif the KXXN variant as present in the *tel* mutant (Fig. S2); nevertheless, the functional relevance of this natural variant remains to be elucidated. Combined, these data suggest that the D to N substitution may cause TEL to bind to a different set of targets, or, alternatively, it may bind its targets more easily, resulting potentially in a hyperactive protein.

Our genetic analysis revealed that *tel* is a dominant mutant, because the heterozygous *tel* mutant suppressed the production of 2n pollen in the *jas-3* background (Fig. 1f). In contrast to *tel*, a mutant allele containing a T-DNA insertion in the *TEL* coding

© 2022 The Authors
New Phytologist © 2022 New Phytologist Foundation.

14698137, 2023, 4, Downloaded from https://nphonlinelibrary.wiley.com/doi/10.1111/nph.18473 by Swedish University Of Agricultural Sciences, Wiley Online Library on [13/03/2023]. See the Terms and Conditions (https://onlinelibrary.wiley.com/terms-and-conditions) on Wiley Online Library for rules of use; OA articles are governed by the applicable Creative Commons License

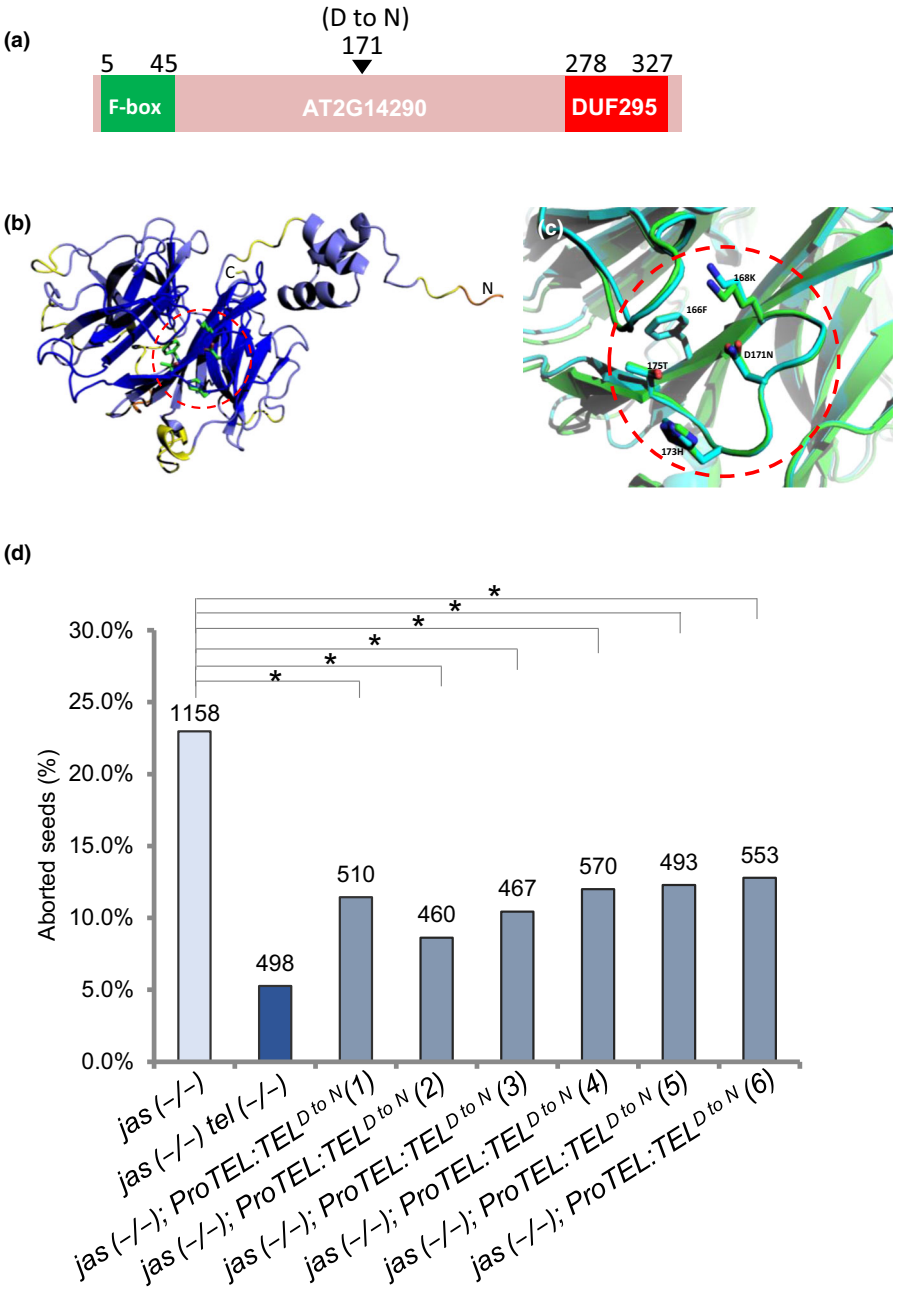

Fig. 4 *TELAMON (TEL)* encodes an F-box domain-containing protein in *Arabidopsis thaliana*. (a) Structure and sites of mutations in TEL. (b) Alpha-fold prediction of the TEL protein. The predicted protein pocket impacted by the D171N mutation is highlighted with a red circle. Residues are colour coded with per-residue confidence score (pLDDT). Dark blue: very high (pLDDT > 90), light blue: confident (90 > pLDDT > 70), yellow: low (70 > pLDDT > 50), orange: very low (pLDDT < 50). (c) Overlay of predicted structures of the TEL WT (green) and TEL mutant (blue) protein pocket. The D171N mutation reduces the electrostatic interaction between 171D and 168K, increasing the distance between the amino acid side chains and resulting in the formation of an enlarged pocket. (d) Percentage of aborted seeds in *jason (jas) (−/−)*, *jas (−/−) tel (−/−)*, and *jas (−/−)* T1 lines expressing *TEL* with the 171 D to N substitution ($TEL^{D\ to\ N}$) under control of the *TEL* promoter. Six independent T1 lines were analyzed. Numbers on top of the bars correspond to the numbers of analyzed seeds. Asterisks mark indicated the difference between T1 lines and *jas* are significant (Chi-square test, $P < e{-}08$).

region (*tel-2*) did not rescue the *jas* mutant seed abortion phenotype (Fig. S3), consistent with *tel* being a dominant gain-of-function mutant. To confirm the identified mutation is indeed the cause for the *tel* mutant phenotype, we introduced a construct containing the promoter and coding region of *At2g14290* with the *tel* point mutation (*ProTEL:*$TEL^{D\ to\ N}$) into the *jas* background and tested whether it could mimic the *tel* phenotype. Indeed, *jas* mutants expressing *ProTEL:*$TEL^{D\ to\ N}$ formed significantly fewer aborted seeds compared to *jas* (Fig. 4d). Hence, we conclude that the mutation in *At2g14290* is responsible for the *tel* mutant phenotype.

Based on publicly available expression data, *TEL* is highly expressed in roots, but also in other plant organs including flowers, stamen and pollen (Fig. S4). We generated reporter constructs expressing TEL and $TEL^{D\ to\ N}$ fused to GFP under control of the native *TEL* promoter. However, we failed to detect GFP fluorescence in anthers in transgenic lines expressing both constructs (not shown), suggesting that TEL accumulates below detection levels. Based on the prediction using SUBA4 (Hooper *et al.*, 2017), Plant-mPLoc (Chou & Shen, 2010), and WoLFPSORT (Horton *et al.*, 2007), TEL is most likely located in the cytoplasm and nucleus. To experimentally test TEL's subcellular localization, we generated reporter constructs expressing TEL and $TEL^{D\ to\ N}$ fused to GFP under the control of the *UBQ* promoter and transiently expressed then in tobacco leaves. In line with the prediction, a strong GFP signal was detected in the nucleus and cytoplasm with both, TEL-GFP and $TEL^{D\ to\ N}$-GFP constructs (Fig. S5a–f), indicating a functional role of TEL

© 2022 The Authors
New Phytologist © 2022 New Phytologist Foundation.

14698137, 2023, 4, Downloaded from https://nphonlinelibrary.wiley.com/doi/10.1111/nph.18473 by Swedish University Of Agricultural Sciences, Wiley Online Library on [13/03/2023]. See the Terms and Conditions (https://onlinelibrary.wiley.com/terms-and-conditions) on Wiley Online Library for rules of use; OA articles are governed by the applicable Creative Commons License

in nucleus and cytoplasm. Given that F-box proteins are generally involved in protein degradation, we propose that gain of TEL function may cause degradation of proteins that restrict meiocyte size.

Discussion

Our study revealed that enlarged meiocytes can bypass the requirement of the organelle band to maintain spindle separation during meiosis II, unravelling a thus far unknown connection between the organelle band and meiocyte size. Mutants in *EXCESS MICROSPOROCYTES1* (*EMS1*) and *TAPETUM DETERMINANT1* (*TPD1*) form excess microspores (Zhao *et al.*, 2002; Yang *et al.*, 2003), indicating that the number of meiocytes and thus the number of pollen is genetically controlled. As the number and size of pollen are inversely correlated (Cruden & Miller-Ward, 1981; Vonhof & Harder, 1995), we speculate that meiocyte size determines pollen size and final pollen number. There is strong variation in pollen size among plant species, which is considered a consequence of strong selection pressures on pollen dispersal strategies (Knight *et al.*, 2010). While wind-pollinated species frequently form small and light pollen, insect-pollinated species have large variation in pollen size (Knight *et al.*, 2010; Cruden, 2000). However, given a size-number trade-off in pollen, small pollen is considered to be evolutionarily favoured (Knight *et al.*, 2010).

The majority of dicotyledonous plants undergo simultaneous male meiotic cytokinesis, where cytokinesis takes place only after the completion of the second meiotic division (Brownfield & Kohler, 2011; De Storme & Geelen, 2013). If meiotic cell size decreases, the two groups of chromosomes separated in meiosis I are closer to each other, risking interactions between these groups. The organelle band, which is formed in the middle of meiotic cells at metaphase II, acts as a physical barrier and is essential for keeping the spindles and chromosome groups physically separated at metaphase II (Brownfield *et al.*, 2015). We thus propose that the organelle band is particularly important in small meiocytes, where space constraints bring separated chromosomes in close proximity at meiosis II. This view is strongly supported by our data showing that increase of meiocyte size allows bypassing the requirement of the organelle band. Like the *jas tel* mutant, 4× *jas* mutants formed strongly enlarged meiocytes that despite having no organelle band were able to keep most chromosome groups separated at meiosis II and form reduced gametes. Nevertheless, despite 4× *jas* forming larger meiocytes than *jas tel*, it formed more triads than *jas tel*. Since the chromosome number in 4× *jas* is twice that of *jas tel*; we propose that the requirement of the organelle band depends on the ratio of meiotic cell size and chromosome number. TEL is an F-box protein that usually function in protein degradation. The gain-of-function mutation of *tel* causes increased meiocyte size, suggesting that $TEL^{D\ to\ N}$ degrades proteins restricting meiocyte size. Interestingly, the *tel*-mediated increase in meiocyte size was dependent on the *jas* mutation. Possibly, the connection between non-degraded inhibitors of cell size regulation (due to the *tel* mutation) and the availability of endomembrane vesicles that are otherwise located in the organelle band (due to the *jas* mutation) allow increase of meiocyte size. Testing this model and identifying the targets of $TEL^{D\ to\ N}$ will be subject of future studies. Moreover, given that the substitution of 171D to 171N naturally occurs in several Brassicaceae species (Fig. S5), it will be interesting to test if this natural variant impacts on meiocyte size and frequency of unreduced gametes in different species.

Together, our study generates novel insights into the role of meiocyte size for successful meiosis and the requirement of the organelle band as a possible means to enable a decrease in meiocyte size and thus increase pollen number, while still largely producing reduced pollen.

Acknowledgements

This research was supported by a research grant from the Swedish Research Council VR (to CK), and a grant from the DFG to HJ (JI 347/5-1). Open Access funding enabled and organized by Projekt DEAL.

Author contributions

JY, CK, LB and HJ designed the research and wrote the manuscript. YJ, DK, YM, EP and LB executed the experimental procedures. All authors discussed the results and commented on the manuscript.

ORCID

Lynette Brownfield https://orcid.org/0000-0002-3490-5444
Hua Jiang https://orcid.org/0000-0002-7561-3085
Claudia Köhler https://orcid.org/0000-0002-2619-4857
Yingrui Ma https://orcid.org/0000-0002-2287-5321
Ewa Piskorz https://orcid.org/0000-0002-4752-6822
Jun Yi https://orcid.org/0000-0001-5539-0016

Data availability

All data and material that support the findings of this study are available upon request from the corresponding authors.

References

Armstrong SJ, Jones GH. 2003. Meiotic cytology and chromosome behaviour in wild-type *Arabidopsis thaliana*. *Journal of Experimental Botany* **54**: 1–10.

Arnold B, Kim ST, Bomblies K. 2015. Single geographic origin of a widespread autotetraploid *Arabidopsis arenosa* lineage followed by interploidy admixture. *Molecular Biology and Evolution* **32**: 1382–1395.

Batista RA, Figueiredo DD, Santos-Gonzalez J, Kohler C. 2019. Auxin regulates endosperm cellularization in *Arabidopsis*. *Genes & Development* **33**: 466–476.

Bleckmann A, Alter S, Dresselhaus T. 2014. The beginning of a seed: regulatory mechanisms of double fertilization. *Frontiers in Plant Science* **5**: 1–12.

Brownfield L, Kohler C. 2011. Unreduced gamete formation in plants: mechanisms and prospects. *Journal of Experimental Botany* **62**: 1659–1668.

Brownfield L, Yi J, Jiang H, Minina EA, Twell D, Kohler C. 2015. Organelles maintain spindle position in plant meiosis. *Nature Communications* **6**: 6492.

Cardozo T, Pagano M. 2004. The SCF ubiquitin ligase: insights into a molecular machine. *Nature Reviews Molecular Cell Biology* **5**: 739–751.

© 2022 The Authors
New Phytologist © 2022 New Phytologist Foundation.

14698137, 2023, 4, Downloaded from https://nphonlinelibrary.wiley.com/doi/10.1111/nph.18473 by Swedish University Of Agricultural Sciences, Wiley Online Library on [13/03/2023]. See the Terms and Conditions (https://onlinelibrary.wiley.com/terms-and-conditions) on Wiley Online Library for rules of use; OA articles are governed by the applicable Creative Commons License

14698137, 2023, 4, Downloaded from https://nphonlinelibrary.wiley.com/doi/10.1111/nph.18473 by Swedish University Of Agricultural Sciences, Wiley Online Library on [13/03/2023]. See the Terms and Conditions (https://onlinelibrary.wiley.com/terms-and-conditions) on Wiley Online Library for rules of use; OA articles are governed by the applicable Creative Commons License

Chou KC, Shen HB. 2010. Plant-mPLoc: a top-down strategy to augment the power for predicting plant protein subcellular localization. *PLoS ONE* **5**: e11335.

Cruden RW. 2000. Pollen grains: why so many? *Plant Systematics and Evolution* **222**: 143–165.

Cruden RW, Miller-Ward S. 1981. Pollen-ovule ratio, pollen size, and the ratio of stigmatic area to the pollen-bearing area of the pollinator: an hypothesis. *Evolution* **35**: 964–974.

De Storme N, Geelen D. 2011. The Arabidopsis mutant *jason* produces unreduced first division restitution male gametes through a parallel/fused spindle mechanism in meiosis II. *Plant Physiology* **155**: 1403–1415.

De Storme N, Geelen D. 2013. Sexual polyploidization in plants cytological mechanisms and molecular regulation. *New Phytologist* **198**: 670–684.

d'Erfurth I, Jolivet S, Froger N, Catrice O, Novatchkova M, Mercier R. 2009. Turning meiosis into mitosis. *PLoS Biology* **7**: e1000124.

d'Erfurth I, Jolivet S, Froger N, Catrice O, Novatchkova M, Simon M, Jenczewski E, Mercier R. 2008. Mutations in *AtPS1* (*Arabidopsis thaliana parallel spindle 1*) lead to the production of diploid pollen grains. *PLoS Genetics* **4**: e1000274.

Douglas GM, Gos G, Steige KA, Salcedo A, Holm K, Josephs EB, Arunkumar R, Agren JA, Hazzouri KM, Wang W *et al.* 2015. Hybrid origins and the earliest stages of diploidization in the highly successful recent polyploid *Capsella bursa-pastoris*. *Proceedings of the National Academy of Sciences, USA* **112**: 2806–2811.

Erilova A, Brownfield L, Exner V, Rosa M, Twell D, Scheid OM, Hennig L, Kohler C. 2009. Imprinting of the polycomb group gene *MEDEA* serves as a ploidy sensor in Arabidopsis. *PLoS Genetics* **5**: e1000663.

Grefen C, Donald N, Hashimoto K, Kudla J, Schumacher K, Blatt MR. 2010. A ubiquitin-10 promoter-based vector set for fluorescent protein tagging facilitates temporal stability and native protein distribution in transient and stable expression studies. *The Plant Journal* **64**: 355–365.

Hamamura Y, Nagahara S, Higashiyama T. 2012. Double fertilization on the move. *Current Opinion in Plant Biology* **15**: 70–77.

Henry IM, Dilkes BP, Young K, Watson B, Wu H, Comai L. 2005. Aneuploidy and genetic variation in the *Arabidopsis thaliana* triploid response. *Genetics* **170**: 1979–1988.

Hooper CM, Castleden IR, Tanz SK, Aryamanesh N, Millar AH. 2017. SUBA4: the interactive data analysis centre for Arabidopsis subcellular protein locations. *Nucleic Acids Research* **45**: D1064–D1074.

Horton P, Park KJ, Obayashi T, Fujita N, Harada H, Adams-Collier CJ, Nakai K. 2007. WoLF PSORT: protein localization predictor. *Nucleic Acids Research* **35**: W585–W587.

Jumper J, Evans R, Pritzel A, Green T, Figurnov M, Ronneberger O, Tunyasuvunakool K, Bates R, Zidek A, Potapenko A *et al.* 2021. Highly accurate protein structure prediction with AlphaFold. *Nature* **596**: 583–589.

Knight CA, Clancy RB, Götzenberger L, Dann L, Beaulieu JM. 2010. On the relationship between pollen size and genome size. *Journal of Botany* **2010**: 612017.

Kradolfer D, Wolff P, Jiang H, Siretskiy A, Kohler C. 2013. An imprinted gene underlies postzygotic reproductive isolation in *Arabidopsis thalia*na. *Development Cell* **26**: 525–535.

Lama S, Broda M, Abbas Z, Vaneechoutte D, Belt K, Säll T, Vandepoele K, Aken OV. 2019. Neofunctionalization of mitochondrial proteins and incorporation into signaling networks in plants. *Molecular Biology and Evolution* **36**: 974–989.

Li Y, Shen Y, Cai C, Zhong C, Zhu L, Yuan M, Ren H. 2010. The type II Arabidopsis formin14 interacts with microtubules and microfilaments to regulate cell division. *Plant Cell* **22**: 2710–2726.

Ma H. 2006. A molecular portrait of *Arabidopsis meiosis*. *Arabidopsis Book* **4**: e0095.

Martin K, Kopperud K, Chakrabarty R, Banerjee R, Brooks R, Goodin MM. 2009. Transient expression in *Nicotiana benthamiana* fluorescent marker lines provides enhanced definition of protein localization, movement and interactions in planta. *The Plant Journal* **59**: 150–162.

Novikova PY, Hohmann N, Van de Peer Y. 2018. Polyploid *Arabidopsis* species originated around recent glaciation maxima. *Current Opinion in Plant Biology* **42**: 8–15.

Orr-Weaver TL. 2015. When bigger is better: the role of polyploidy in organogenesis. *Trends in Genetics* **31**: 307–315.

Ramsey J, Schemske DW. 1998. Pathways, mechanisms, and rates of polyploid formation in flowering plants. *Annual Review of Ecology and Systematics* **29**: 467–501.

Rossig C, Le Lievre L, Pilkington SM, Brownfield L. 2021. A simple and rapid method for imaging male meiotic cells in anthers of model and non-model plant species. *Plant Reproduction* **34**: 37–46.

Schatlowski N, Kohler C. 2012. Tearing down barriers: understanding the molecular mechanisms of interploidy hybridizations. *Journal of Experimental Botany* **63**: 6059–6067.

Varadi M, Anyango S, Deshpande M, Nair S, Natassia C, Yordanova G, Yuan D, Stroe O, Wood G, Laydon A *et al.* 2022. AlphaFold protein structure database: massively expanding the structural coverage of protein-sequence space with high-accuracy models. *Nucleic Acids Research* **50**: D439–D444.

Vonhof MJ, Harder LD. 1995. Size-number trade-offs and pollen production by papilionaceous legumes. *American Journal of Botany* **82**: 230–238.

Xiao W, Jang J. 2000. F-box proteins in Arabidopsis. *Trends in Plant Science* **5**: 454–457.

Yang SL, Xie LF, Mao HZ, Puah CS, Yang WC, Jiang L, Sundaresan V, Ye D. 2003. *TAPETUM DETERMINANT1* is required for cell specialization in the Arabidopsis anther. *Plant Cell* **15**: 2792–2804.

Zamariola L, Tiang CL, De Storme N, Pawlowski W, Geelen D. 2014. Chromosome segregation in plant meiosis. *Frontiers in Plant Science* **5**: 279.

Zhao DZ, Wang GF, Speal B, Ma H. 2002. The *EXCESS MICROSPOROCYTES1* gene encodes a putative leucine-rich repeat receptor protein kinase that controls somatic and reproductive cell fates in the *Arabidopsis* anther. *Genes and Development* **16**: 2021–2031.

Supporting Information

Additional Supporting Information may be found online in the Supporting Information section at the end of the article.

Fig. S1 Male meiosis in 4× *Arabidopsis thaliana* accession Wa-1, 4× *Arabidopsis arenosa*, and 4× *Capsella bursa pastoris*.

Fig. S2 Alignment of TEL and its homologs in other Brassicaceae species.

Fig. S3 Percentage of collapsed seeds in *jas (−/−)* and *jas (−/−) tel-2 (−/−)*.

Fig. S4 Expression of TEL in different plant tissues.

Fig. S5 Localization of transiently expressed TEL-GFP and $TEL^{D\ to\ N}$-GFP in tobacco leaves.

Table S1 List of primers used in this study.

Table S2 Analysis of the area including 171D and 168K among the homologs of TEL in *Arabidopsis thaliana* and multiple Brassicaceae species.

Please note: Wiley is not responsible for the content or functionality of any Supporting Information supplied by the authors. Any queries (other than missing material) should be directed to the *New Phytologist* Central Office.

© 2022 The Authors
New Phytologist © 2022 New Phytologist Foundation.